

---

# Estimating Heterogeneous Treatment Effects by Combining Weak Instruments and Observational Data

---

Miruna Oprescu  
Cornell University  
amo78@cornell.edu

Nathan Kallus  
Cornell University  
kallus@cornell.edu

## Abstract

Accurately predicting conditional average treatment effects (CATEs) is crucial in personalized medicine and digital platform analytics. Since often the treatments of interest cannot be directly randomized, observational data is leveraged to learn CATEs, but this approach can incur significant bias from unobserved confounding. One strategy to overcome these limitations is to seek latent quasi-experiments in instrumental variables (IVs) for the treatment, for example, a randomized intent to treat or a randomized product recommendation. This approach, on the other hand, can suffer from low compliance, *i.e.*, IV weakness. Some subgroups may even exhibit zero compliance meaning we cannot instrument for their CATEs at all. In this paper we develop a novel approach to combine IV and observational data to enable reliable CATE estimation in the presence of unobserved confounding in the observational data and low compliance in the IV data, including no compliance for some subgroups. We propose a two-stage framework that first learns *biased* CATEs from the observational data, and then applies a compliance-weighted correction using IV data, effectively leveraging IV strength variability across covariates. We characterize the convergence rates of our method and validate its effectiveness through a simulation study. Additionally, we demonstrate its utility with real data by analyzing the heterogeneous effects of 401(k) plan participation on wealth.

## 1 Introduction

The use of observational data to perform individual-level causal analyses is increasingly commonplace across personalized medicine and online platforms and whenever understanding individualized responses is crucial and/or there is an opportunity to personalize. The key quantity for such analyses is the conditional average treatment effects (CATEs), given baseline covariates (features) with respect to which we want to understand heterogeneity and/or personalize.

Using observational data can nonetheless introduce bias from unobserved confounding, where the observed dependence between outcomes and interventions is not due solely to treatment effects but also to variables that influence both outcome and treatment and are not controlled for by baseline covariates, such as socioeconomic status, healthfulness, busyness, *etc.* These biases can skew causal effect estimates, resulting in unreliable analysis or even harmful decisions.

Randomized trials are the gold standard for causal inference but are often infeasible. For example, digital services cannot compel a user to see/try/buy a product and clinical trials may not force invasive treatments. An alternative is randomizing the encouragement toward certain actions, such as recommending a product/treatment. These randomized encouragements can serve as instrumental variables (IVs). Under certain conditions, IVs can enable unbiased treatment effect estimation [4].

Identification of CATEs using on IVs crucially hinges on the premise that compliance – the correlation between the treatment received and the intent/encouragement – is nonzero across all baseline-covariate values. And, whenever compliance is nonzero but small, estimation based on IVs exhibits high

variance and can become unreliable [3]. In practice, the assumption of strong compliance is often violated. For example, certain users on digital platforms may disregard recommendations either altogether or of certain undesired content, and on mobile health platforms certain participants may ignore recommendations (*e.g.* taking 250 steps per hour) due to time constraints or disinterest.

To address the challenge of estimating unbiased CATEs in the presence of unobserved confounding and low compliance, we introduce a two-stage framework. In the first stage, we identify a confounded CATE from observational data. Then, in the second stage, we utilize an IV to learn the confounding bias by weighting the samples according to compliance. Assuming only that the bias can be extrapolated, this method extends treatment effect adjustments to those minimally influenced by the IV, employing a transfer learning approach that leverages varying instrument strengths across covariate groups.

This framework mirrors strategies in causal inference that combine randomized trials with observational data to manage low covariate overlap. Building on this body of work, we introduce two methodologies for extrapolating confounding bias within the observational dataset: a parametric estimation approach, assuming the confounding bias adheres to a parametric form, and a transfer learning strategy that assumes a shared representation between the true and biased CATE. We study the properties of our CATE estimators in finite samples and validate our approaches through comprehensive empirical studies.

## 2 Related Work

We briefly overview related work here; for a more comprehensive discussion, refer to Appendix A.

**Heterogeneous treatment effect estimation from observational data:** Recent advances in machine learning have expanded the use of observational data to estimate CATEs using diverse techniques such as random forests [46], Bayesian algorithms [21], deep learning [43], and meta-learners [30]. However, these methods often unrealistically assume an absence of confounding, limiting their real-world applicability.

**Heterogeneous treatment effect estimation using IVs:** Integrating machine learning with instrumental variable (IV) methods enhances CATE estimation flexibility over traditional approaches. Techniques range from advanced two-stage least squares (2SLS) that incorporate complex feature mappings via kernel methods [44] and deep learning [49] to neural networks for conditional density estimation [18] and moment conditions for IV estimation [7]. Yet, these rely on the consistent relevance of instruments across covariate groups, which is not guaranteed with weak instruments.

**Treatment Effect Estimation with Weak Instruments:** Traditional IV methods like 2SLS can be unreliable when instruments are weak, leading to biased, high-variance estimates. Recent advancements include novel estimators such as bias-adjusted 2SLS, limited information maximum likelihood, and jackknife IV estimators (see [22] and references therein). Other techniques attempt to reduce variance by exploiting first-stage heterogeneity (variation in compliance) [1, 11]. Some approaches also combine multiple weak instruments into robust composites, useful in settings like genetic studies [27]. Our approach extends [1, 11] by leveraging compliance weighting to estimate heterogeneous effects and address weak instruments using additional observational data.

**Combining observational and randomized data:** Increasing research focuses on merging observational datasets with randomized control trial (RCT) data to reduce observational bias. Strategies range from imposing structural assumptions such as strong parametric assumptions [26] or a shared structure between the biased and unbiased CATE functions [20], to optimizing dual estimators from both data types for improved bias correction [50]. Our work aligns with efforts to debias treatment effects using both observational and experimental data, but addresses additional challenges such as low compliance, the need to debias the overall effect function rather than individual outcome functions, and the complexity of estimating CATE from IV data using a ratio estimator.

**Where our work lies:** To the best of our knowledge, no current estimation technique effectively combines an IV study, particularly one with weak instruments or low compliance, with an observational study to derive robust and unbiased conditional average treatment effects (CATE) estimates. We bridge this gap by introducing two robust and consistent CATE estimation techniques, building upon previous work on combining RCT and observational data [20, 26], as well as work that addresses the complexities associated with weak instruments [1, 11].

### 3 Background and Setup

We consider the standard setting of causal inference where we aim to learn the conditional average treatment effect of a binary treatment  $A \in \{0, 1\}$  on an outcome  $Y \in \mathbb{R}$  in the presence of covariates  $X \in \mathcal{X} \subseteq \mathbb{R}^m$ . Our approach is grounded in Rubin’s potential outcomes framework, wherein each unit is associated with two potential outcomes  $Y(0), Y(1)$  of which only  $Y = Y(A)$  is observed (causal consistency). Our objective is to learn the CATE function, which is given by:

$$\tau(x) = \mathbb{E}[Y(1) - Y(0) \mid X = x]. \quad (1)$$

However, we only have access to  $n_O$  i.i.d. samples from an observational dataset  $O = (X_i^O, A_i^O, Y_i^O)_{i=1}^{n_O} \sim (X^O, A^O, Y^O)$ . Thus, we are faced with the fundamental problem of causal inference in that we do not observe both potential outcomes, but only the outcome under the administered treatment. Without further assumptions, there exists the possibility of unobserved confounding, leading to a situation where

$$\tau^O(x) = \mathbb{E}[Y^O \mid A^O = 1, X^O = x] - \mathbb{E}[Y \mid A^O = 0, X^O = x] \neq \tau(x), \quad (2)$$

indicating a persistent bias in the observed treatment effects that remains unaffected by increasing the data sample size. We denote this bias by  $b(x)$ . *i.e.*:

$$b(x) = \tau(x) - \tau^O(x).$$

Assuming this bias is induced by a set of unobserved confounders  $U \subseteq \mathbb{R}^k$ , the discrepancy arises because the selection into treatment in the observational population is influenced by  $U$ , which also impacts the outcome  $Y^O$ . Our goal is to mitigate this bias by leveraging additional data.

Alongside the observational dataset, we have  $n_E$  i.i.d. samples from an experimental, intent-to-treat dataset  $E = (X_i^E, Z_i^E, A_i^E, Y_i^E)_{i=1}^{n_E} \sim (X^E, Z^E, A^E)$  with a binary instrument  $Z^E \in \{0, 1\}$ . We also let  $X^E \in \mathcal{X}$  and  $p_{X^E}(x) = p_{X^O}(x)$ , where  $p_X$  denotes the density of the random variable  $X$ . Similar to before, use  $Y^E(A, Z)$  to denote the potential outcome with treatment  $A$  and instrument  $Z$ . Furthermore, let  $A^E(Z)$  denote the potential treatment under instrument  $Z$ . We assume that this dataset obeys the following standard IV assumptions on the data generating process:

**Assumption 1** (Standard IV Assumptions). *We assume the following properties hold: (Exclusion)  $Y^E(A, Z) = Y^E(A)$ , *i.e.* the instrument affects the outcome only through the treatment; (Independence)  $Z \perp U \mid X$  for any unobserved confounder  $U$ ; and (Relevance) there exists a subset  $\mathcal{X}' \subseteq \mathcal{X}$  with non-zero measure such that  $Z^E \not\perp A^E \mid X^E$  for  $X^E \in \mathcal{X}'$ .*

**Assumption 2** (Unconfounded Compliance [47]). *Define the compliance factor  $C$  as  $C := \mathbb{I}[A^E(1) > A^E(0)]$ . Then  $Y^E(1) - Y^E(0) \perp C \mid X^E$ .*

We note that the relevance assumption in Assumption 1 is a weaker version of the standard IV assumptions since we allow for arbitrarily weak instruments in some regions of the covariate spaces. With Assumption 1 and Assumption 2, we can identify the CATE as:

$$\tau^E(x) = \frac{\mathbb{E}[Y^E \mid Z^E = 1, X^E = x] - \mathbb{E}[Y^E \mid Z^E = 0, X^E = x]}{\mathbb{E}[A^E \mid Z^E = 1, X^E = x] - \mathbb{E}[A^E \mid Z^E = 0, X^E = x]} := \frac{\delta_Y(x)}{\gamma(x)} = \tau(x) \quad (3)$$

for  $x \in \mathcal{X}'$ . Here,  $\gamma(x)$  denotes heterogeneous compliance, a measure of instrument strength, given by  $\gamma(x) = P(C = 1 \mid X^E = x)$  under Assumption 2. A *strong* instrument ( $\gamma(x) \rightarrow 1$ ) indicates high adherence to the recommended treatment, with  $\gamma(x) = 1$  signifying perfect compliance, similar to a true randomized controlled trial (RCT). Conversely, a *weak* instrument ( $\gamma(x) \rightarrow 0$ ) suggests minimal influence on treatment uptake, with  $\gamma(x) = 0$  indicating no compliance and a confounded selection into treatment. The relevance assumption in Assumption 1 ensures  $\gamma(x) > 0$  for  $x' \in \mathcal{X}'$ , validating the estimation procedure in Equation 3. However, small  $\gamma(x)$  values lead to estimates of  $\tau(x)$  with high asymptotic variance. Moreover, we wish to extend  $\tau(X)$  estimation from  $\mathcal{X}'$  to  $\mathcal{X}$ , our population of interest.

Thus, relying solely on observational data results in biased  $\tau(x)$  estimates, while experimental data alone can yield high variance or invalid estimates for  $\tau(x)$  with low compliance. This work seeks to overcome these challenges by strategically combining the strengths of both datasets to provide a robust CATE estimation technique.

**Notation:** We denote the  $L_2$  norm of a function  $f$  as  $\|f\|_{L_2} := \mathbb{E}_F[f(X)^2]^{1/2}$ , and the  $L_2$  Euclidean norm of a vector  $\theta \in \mathbb{R}^d$  as  $\|\theta\|_2$ . The notation  $\hat{f}$  represents the estimated value of a parameter or function, where  $f$  is the true value. We omit the distribution subscript when clear from context; *e.g.*,  $\mathbb{E}[X^E]$  and  $\mathbb{E}[X^O]$  denote expectations over experimental and observational samples, respectively.

## 4 Estimation Method

To obtain robust CATE estimates for the population  $\mathcal{X}$ , we propose a two-step framework that integrates information from both the observational data and the IV study. First, we learn the confounded CATE function  $\hat{\tau}^O(x)$  using the observational data  $(X_i^O, A_i^O, Y_i^O)_{i=1}^{n_O}$ . This is a common estimation problem in both causal inference and machine learning and can be addressed with many existing techniques including meta-learners ([30]), random forests ([46]), and neural networks ([43]).

Next, we wish to utilize the learned  $\hat{\tau}^O(x)$  to approximate the bias function  $b(x) = \tau(x) - \tau^O(x)$ . Without oracle access to the true CATE function  $\tau(x)$ , we instead use samples from the experimental (IV) study  $(X_i^E, A_i^E, Y_i^E)_{i=1}^{n_E}$  for which we can estimate an unbiased, but potentially high variance CATE on the compliers. Our data combination strategy hinges on the following lemma:

**Lemma 1.** [CATE Estimation with IVs] *Let  $\pi_Z(x) := P(Z^E = 1 \mid X^E = x)$  be the instrument propensity. Then, the following identity holds for every  $x \in \mathcal{X}'$ :*

$$\mathbb{E} \left[ \frac{Y^E Z^E}{\pi_Z(x)\gamma(x)} - \frac{Y^E(1 - Z^E)}{(1 - \pi_Z(x))\gamma(x)} \mid X^E = x \right] = \tau(x)$$

We note that in the case of randomized instrument assignment, the instrument propensity is known and often given by a constant, i.e.  $\pi_Z(x) = \pi_Z > 0$ . Letting  $V_Z(x) = \pi_Z(x)(1 - \pi_Z(x))$ , Lemma 1 indicates that we can learn  $\gamma(x)$  and, if necessary,  $\pi_Z(x)$  from data and utilize the pseudo-outcome

$$\frac{\tilde{Y}^E}{\hat{V}_Z(X^E)\hat{\gamma}(X^E)} := \frac{Y^E Z^E(1 - \hat{\pi}_Z(X^E)) - Y^E(1 - Z^E)\hat{\pi}_Z(X^E)}{\hat{V}_Z(X^E)\hat{\gamma}(X^E)}$$

in subsequent regression tasks to obtain an unbiased estimate of  $\tau(x)$  for  $x \in \mathcal{X}'$  (provided  $\pi_Z$  and  $\gamma$  are estimated consistently). However, such an estimator requires precise knowledge of the population  $\mathcal{X}'$  where  $\gamma(x) > 0$ . Additionally, for small values of  $\gamma(x)$ ,  $\pi_Z(x)$ , and  $1 - \pi_Z(x)$ , this method may result in high variance in the estimates of  $\hat{b}(x)$ , especially for certain parametric function classes. To address these challenges, we weight the data samples by the inverse variance of  $\tilde{Y}^E/(\hat{\gamma}(x)\hat{V}_Z(x))$  given by  $\text{Var}(\tilde{Y}^E \mid X^E = x)^{-1} \hat{\gamma}^2(x) \hat{V}_Z^2(x)$ . This approach is frequently used in generalized least squares methods (GLS, [2]) to confer the algorithm asymptotic efficiency. While  $\text{Var}(\tilde{Y}^E \mid X^E = x)$  can be estimated from data using machine learning methods, it is generally preferable to weigh the estimator solely by compliance and instrument propensity to avoid issues with large values of  $\text{Var}(\tilde{Y}^E \mid X^E = x)^{-1}$ . Assuming the bias function belongs to a class of functions  $\mathcal{B}$ , our proposed algorithm can be described by the following weighted empirical risk minimization (ERM) procedure.

$$\hat{b} = \arg \min_{b \in \mathcal{B}} \sum_{i=1}^{n_E} \left( \tilde{Y}_i^E - \hat{\gamma}(X_i^E) \hat{V}_Z(X_i^E) \hat{\tau}^O(X_i^E) - \hat{\gamma}(X_i^E) \hat{V}_Z(X_i^E) b(X_i^E) \right)^2 \quad (4)$$

where the factor  $\hat{\gamma}^2(x) \hat{V}_Z^2(x)$  was used for weighting the squared loss. This estimator automatically eliminates the need to know  $\mathcal{X}'$  since we assign weights of 0 when  $\hat{\gamma} = 0$ . Moreover, this method places higher emphasis on lower-variance pseudo-outcomes, thereby minimizing the risk of overfitting to data points with high variance. This technique is commonly employed in other IV estimation tasks, such as local *average* treatment effect estimation (LATE), where weighting data points by compliance yields estimators with lower variance ([1, 11]).

The weighting scheme in Equation 4 creates a weighted distribution,  $\tilde{p}_{X^E}(x)$ , for optimizing the ERM procedure. Since  $\tilde{p}_{X^E}(x)$  differs from the target distribution  $p_{X^E}(x)$ , this creates a transfer learning challenge. Without additional constraints on the function class  $\mathcal{B}$ , the minimization in Equation 4 may yield many possible solutions. To ensure a unique or limited solution set,  $\mathcal{B}$  must have low complexity or require further structural assumptions. We explore two function classes within  $\mathcal{B}$ : a parametric class defined by  $b(x) = \theta^T \phi(x)$  with a known mapping  $\phi : \mathcal{X} \rightarrow \mathbb{R}^d$ , and another parametric class where  $b(x) = \nu^T \phi(x)$  uses  $\phi \in \Phi$ , a learned representation common to both the observational and IV datasets.

### 4.1 Integrating Observational and Experimental Data via Parametric Extrapolation

We consider parametric classes  $\mathcal{B}_\phi = \{\theta^T \phi(x) : \theta \in \mathbb{R}^d\}$  for a known mapping  $\phi : \mathcal{X} \rightarrow \mathbb{R}^d$ . Since the compliance factor  $\gamma(x)$ , instrument propensity  $\pi_Z(x)$ , and the parameter of interest  $\theta^T$  are

---

**Algorithm 1** CATE Estimation with Parametric Extrapolation
 

---

- 1: **Input:** Observational dataset  $O = (X_i^O, A_i^O, Y_i^O)_{i=1}^{n_O}$ , IV dataset  $E = (X_i^E, Z_i^E, A_i^E, Y_i^E)_{i=1}^{n_E}$ ,  $\tau^O(x)$  estimator  $\mathcal{T}$ ,  $\gamma(x)$  estimator  $\mathcal{G}$ ,  $\pi_Z(x)$  estimator  $\mathcal{P}$ , known mapping  $\phi : \mathcal{X} \rightarrow \mathbb{R}^d$ .
  - 2: Learn  $\hat{\tau}^O(x)$  using  $\mathcal{T}$  on  $O$ . Let  $\tilde{\mathbf{Y}} \in \mathbb{R}^d$ ,  $\tilde{\mathbf{X}} \in \mathbb{R}^{n \times d}$ .
  - 3: **for**  $k = 1, 2, \dots, K$  **do**
  - 4:   Set  $\mathcal{I}_k = \{i \in \{1, \dots, n_E\} : i = k - 1 \pmod{K}\}$ .
  - 5:   Use data  $\{(X_i^E, Z_i^E, A_i^E, Y_i^E) \in E : i \notin \mathcal{I}_k\}$  to learn  $\hat{\gamma}^{(k)}(x)$  with  $\mathcal{G}$  and  $\hat{\pi}_Z^{(k)}(x)$  with  $\mathcal{P}$ .
  - 6:   **for**  $i = k - 1 \pmod{K}$  **do**
  - 7:     Set  $\tilde{\mathbf{Y}}_i = Y_i^E Z_i^E (1 - \hat{\pi}_Z^{(k)}(X_i^E)) - Y_i^E (1 - Z_i^E) \hat{\pi}_Z^{(k)}(X_i^E) - \hat{w}^{(k)}(X_i^E) \hat{\tau}^O(X_i^E)$ .
  - 8:     Set  $\tilde{\mathbf{X}}_{ij} = \hat{w}^{(k)}(X_i^E) \phi_j(X_i^E)$  for each  $j \in \{1, \dots, d\}$ .
  - 9: **Output:**  $\hat{\theta} = (\tilde{\mathbf{X}}^T \tilde{\mathbf{X}})^{-1} \tilde{\mathbf{X}}^T \tilde{\mathbf{Y}}$ .
- 

learned from the same dataset  $E$ , we propose the following  $K$ -fold cross-fitted estimation procedure:

$$\hat{\theta} = \arg \min_{\theta \in \mathbb{R}^d} \sum_{k=1}^K \sum_{i \in \mathcal{I}_k^E} \left( \tilde{Y}_i^E - \hat{w}^{(k)}(X_i^E) \hat{\tau}^O(X_i^E) - \theta^T \hat{w}^{(k)}(X_i^E) \phi(X_i^E) \right)^2 \quad (5)$$

where  $\hat{w}^{(k)}(X_i^E) := \hat{\gamma}^{(k)}(X_i^E) \hat{V}_Z^{(k)}(X_i^E)$ , and the compliance factor  $\hat{\gamma}^{(k)}$  and instrument propensity  $\hat{\pi}_Z^{(k)}$ ,  $k \in [K]$  are trained on  $E$  excluding the  $k^{\text{th}}$  fold containing indices  $\mathcal{I}_k^E$ .  $K$ -fold cross-fitting is crucial because it ensures that the weights are learned from data distinct from that used in the ERM algorithm. This separation is essential for maintaining desirable theoretical properties as we remain methodologically agnostic to the techniques used for learning  $\gamma$  and  $\pi_Z$ .

The compliance factor can be estimated using standard machine learning classification algorithms, either by training separate classifiers for  $E \mid Z = 1$  and  $E \mid Z = 0$  or by using one classifier with  $Z$  as an additional feature. Similarly, instrument propensity estimation is a straightforward classification task with  $Z$  as the target. Given estimates  $\hat{\tau}^O$ ,  $\hat{\gamma}^{(k)}$ , and  $\hat{\pi}_Z^{(k)}$ , the result in is obtained by running an OLS procedure with the target  $\tilde{Y}_i^E - \hat{w}^{(k)}(X_i^E) \hat{\tau}^O(X_i^E)$  and the design matrix  $\tilde{\mathbf{X}} = W(X^E) \Phi(X^E)$ . Here,  $W(X^E) = \text{diag}(\hat{\gamma}(X_1^E) \hat{V}_Z(X_1^E), \dots, \hat{\gamma}(X_{n_E}^E) \hat{V}_Z(X_{n_E}^E))$ , and  $\Phi(X^E) = (\phi(X_1^E), \dots, \phi(X_{n_E}^E))^T$ . The two-step procedure is detailed in Algorithm 1.

Next, we provide theoretical guarantees for our parametric extrapolation approach. We begin by describing the regularity assumptions that enable the consistency of our estimator.

**Assumption 3** (Regularity Assumptions). *The following claims are true:*

1. (Treatment Positivity in  $O$ )  $\epsilon \leq P(A^O = 1 \mid X^O = x) \leq 1 - \epsilon$  for some  $\epsilon > 0$ .
2. (Instrument Positivity)  $\epsilon \leq \pi_Z(X^E), \hat{\pi}_Z(X^E) \leq 1 - \epsilon$  for some  $\epsilon > 0$ .
3. (Boundedness)  $Y^E, Y^O, \|X^E\|_2, \|\phi(X^E)\|_2, \hat{\tau}^O(x), \hat{\gamma}(x)$  are uniformly bounded.
4. (Realizability of  $b(x)$ )  $b(x) \in \mathcal{B}_\phi$ , i.e.  $\tau(x) - \tau^O(x) = \theta^T \phi(x)$ .
5. (Identifiability of  $\theta$ )  $\mathbb{E}[\phi(X^E) \phi(X^E)^T]$  is invertible.

The first two conditions in Assumption 3 are standard in causal inference, ensuring that both treatments (or instruments) and controls are observable for every  $x \in \mathcal{X}$ , enabling CATE estimation. The third condition imposes a common boundedness assumption to control the growth of estimands. The fourth condition ensures our model for the bias function  $b(x)$  is well-specified given  $\mathcal{B}_\phi$ . The final condition requires that the design matrix has rank  $d$ , ensuring we can learn the parameter  $\theta$  from data. Given Assumption 3, we present the following theoretical result:

**Theorem 2** (Estimator Consistency for Parametric Extrapolation). *Let  $r_\gamma(n)$ ,  $r_{\pi_Z}(n)$ , and  $r_{\tau^O}(n)$  be  $o_p(1)$  functions of  $n \in \mathbb{N}$  such that  $\|\gamma - \hat{\gamma}^{(k)}\|_{L_2} \leq r_\gamma(n_E)$ ,  $\|\pi_Z - \hat{\pi}_Z^{(k)}\|_{L_2} \leq r_{\pi_Z}(n_E)$ , and  $\|\tau^O - \hat{\tau}^O\|_{L_2} \leq r_{\tau^O}(n_O)$ . Furthermore, assume the conditions of Assumption 1, Assumption 2, and Assumption 3 hold. Then, the parameter  $\hat{\theta}$  returned by Algorithm 1 is consistent and satisfies*

$$\|\hat{\theta} - \theta\|_2 = O_p(r_\gamma(n_E) + r_{\pi_Z}(n_E) + r_{\tau^O}(n_O) + 1/\sqrt{n_E}).$$

Moreover,  $\hat{\tau}$  is consistent on  $\mathcal{X}$  with convergence rate given by

$$\|\hat{\tau} - \tau\|_{L_2} = O_p(r_\gamma(n_E) + r_{\pi_Z}(n_E) + r_{\tau^O}(n_O) + 1/\sqrt{n_E}).$$

---

**Algorithm 2** CATE Estimation with Representation Learning
 

---

- 1: **Input:** Observational dataset  $O = (X_i^O, A_i^O, Y_i^O)_{i=1}^{n_O}$ , IV dataset  $E = (X_i^E, Z_i^E, A_i^E, Y_i^E)_{i=1}^{n_E}$ ,  $(\phi, h^O)$  estimator  $\mathcal{T}$ ,  $\gamma(x)$  estimator  $\mathcal{G}$ ,  $\pi_Z(x)$  estimator  $\mathcal{P}$ .
  - 2: Learn  $\hat{\phi}(x)$  and  $\hat{h}^O$  using  $\mathcal{T}$  on  $O$ .
  - 3: Call Algorithm 1 with  $\phi = \hat{\phi}$  and  $\hat{\tau}^O(x) = (\hat{h}^O)^T \hat{\phi}(x)$ . Let  $\hat{\nu}$  be its output.
  - 4: **Output:**  $\hat{\nu}$ .
- 

**Remark 1** (Instrument Propensity). *While we describe our estimation technique in full generality, in practice, the instrument propensity  $\pi_Z(x)$  is often known, which significantly streamlines both our estimation procedure and our theoretical results. Specifically, if  $\pi_Z(x)$  is known, there is no need to learn this function from data, and the algorithm’s convergence rates simplify to  $O_p(r_\gamma(n_E) + r_{\tau^O}(n_O) + 1/\sqrt{n_E})$ , which are solely dependent on the rates of the biased CATE  $\hat{\tau}^O$  and the compliance term  $\hat{\gamma}$ .*

We provide the proof of Theorem 2 in Appendix B. The key idea is that weighted OLS remains consistent if the estimates for  $\hat{\gamma}$ ,  $\hat{\pi}_Z$ , and  $\hat{\tau}^O$  are consistent. However, the convergence rate is limited by the slowest rate among them. Typically,  $\pi_Z$  is known, so the convergence rate is mainly influenced by the rate of  $\hat{\gamma}$  and  $\hat{\tau}^O$ . This underscores the trade-off in using both datasets to accurately estimate effects on the target population.

## 4.2 Integrating Observational and Experimental Data via a Common Representation

Without expert knowledge, the mapping  $\phi(x)$  may not be known a priori. In this section, we describe a method to jointly learn the unbiased CATE and the mapping  $\phi(x)$  (referred to as the *representation*) under the assumption that the true CATE  $\tau(x)$  and the biased CATE  $\tau^O(x)$  share a common representation. This approach leverages machine learning techniques that assume a common structure across tasks, such as multi-task and transfer learning. In causal inference, a shared representation may be assumed between treatment arms [42, 43] or between randomized data and confounded observational data [20]. This framework enables us to learn the bias function  $b(x)$  when  $\phi(x) \in \Phi$  is unknown.

We consider a class  $\Phi$  of representations  $\phi(x) : \mathcal{X} \rightarrow \mathbb{R}^d$  and assume there exists a  $\phi \in \Phi$  common to both the true and biased CATEs. Specifically, there are linear hypotheses  $h, h^O \in \mathbb{R}^d$  such that  $\tau(x) = h^T \phi(x)$  and  $\tau^O(x) = (h^O)^T \phi(x)$ , leading to the bias function  $b(x) = (h - h^O)^T \phi(x) := \nu^T \phi(x)$ . For simplicity, we focus on linear-in-representation classes, but more complex hypotheses  $h$  with  $\tau(x) = h(\phi(x))$  can be considered – see [20, 42]. Thus,  $b(x) \in \mathcal{B}_\phi$  for the unknown  $\phi$ , with  $\mathcal{B}_\phi$  defined in Section 4.1. Suppose there exists an ERM algorithm  $\mathcal{T}$  for jointly learning  $\phi(x)$  and  $h^O$  from the observational data,  $O$ . Our learning algorithm proceeds as follows: first, learn  $\hat{\phi}(x)$  and  $\hat{h}^O$  using  $\mathcal{T}$  with  $O$ , along with  $\hat{\gamma}^{(k)}(x)$  and  $\hat{V}^{(k)}(x)$  as described in Section 4.1. In the second stage, we use the following ERM procedure to estimate the parameter  $\nu$ :

$$\hat{\nu} = \arg \min_{\nu \in \mathbb{R}^d} \sum_{k=1}^K \sum_{i \in \mathcal{I}_k^E} \left( \hat{Y}_i^E - (\hat{h}^O)^T \hat{w}^{(k)}(X_i^E) \hat{\phi}(X_i^E) - \nu^T \hat{w}^{(k)}(X_i^E) \hat{\phi}(X_i^E) \right)^2. \quad (6)$$

We detail this procedure in Algorithm 2. We can then recover  $\hat{\tau}(x)$  by setting  $\hat{\tau}(x) = (\hat{h}^O + \hat{\nu})^T \hat{\phi}(x)$ .

**Example 1** (Representation learning with neural networks). *Let  $\Phi$  to be a class of feed-forward neural networks. Then  $\hat{\phi}(x)$ ,  $\hat{h}^O$  and  $\hat{\tau}^O(x)$  can be jointly learned by composing  $\Phi$  with two linear output heads for  $Y^O | A^O = 1, X^O = x$  and  $Y^O | A^O = 0, X^O = x$ , respectively. By taking the difference between the two output heads, we can reconstruct  $\hat{\tau}^O(x)$ , assuming that  $\mathbb{E}[Y^O | A^O = 1, X^O = x]$  and  $\mathbb{E}[Y^O | A^O = 0, X^O = x]$  are also linear in  $\phi$  (see [42, 43]). Without this assumption, we can learn  $\tau^O(x)$  directly by composing  $\Phi$  with one linear output layer and considering the pseudo-outcome  $\frac{Y^O A^O}{\pi_A(X^O)} - \frac{Y^O(1-A^O)}{(1-\pi_A(X^O))}$ . Here,  $\pi_A(X^O) = P(A^O = 1 | X^O)$  is the treatment propensity in  $O$  and can be learned using any black-box machine learning classifier.*

With this setup, we obtain theoretical results similar to those in Theorem 2:

**Theorem 3** (Estimator Consistency for Shared Representation Learning). *Let  $r_\gamma(n)$ ,  $r_{\pi_Z}(n)$ , and  $r_\phi(n)$  be  $o_p(1)$  functions of  $n \in \mathbb{N}$  such that  $\|\gamma - \hat{\gamma}^{(k)}\|_{L_2} \leq r_\gamma(n_E)$ ,  $\|\pi_Z - \hat{\pi}_Z^{(k)}\|_{L_2} \leq r_{\pi_Z}(n_E)$ ,*

and  $\|\phi - \widehat{\phi}\|_{L_2} \leq r_\phi(n_O)$ . Additionally, assume  $\|\widehat{\phi}\|_2$  is bounded and  $\mathbb{E}[\widehat{\phi}(X)\widehat{\phi}(X)^T]$  is invertible. Let us also consider the conditions specified in Assumption 1 and Assumption 2 to be satisfied. Moreover, assume that  $\tau^O(x) = (h^O)^T \phi(x)$  for some  $\phi$  that is realizable within the representation class  $\Phi$  and let Assumption 3 hold for  $\phi$ . Under these conditions, the parameter  $\widehat{\nu}$  returned by Algorithm 2 is consistent and satisfies

$$\|\widehat{\nu} - \nu\|_2 = O_p(r_\gamma(n_E) + r_{\pi_Z}(n_E) + r_\phi(n_O) + 1/\sqrt{n_E} + 1/\sqrt{n_O}).$$

Moreover,  $\widehat{\tau}$  is consistent on  $\mathcal{X}$  with convergence rate given by

$$\|\widehat{\tau} - \tau\|_{L_2} = O_p(r_\gamma(n_E) + r_{\pi_Z}(n_E) + r_\phi(n_O) + 1/\sqrt{n_E} + 1/\sqrt{n_O}).$$

We provide the proof of Theorem 3 in Appendix B. This result relies on the realizability assumption in  $\Phi$  and the linear-in-representation structure of  $\tau$  and  $\tau^O$ . In Example 1,  $r_\phi(n)$  bounds the generalization error for feed-forward neural networks. For ReLU activations and bounded outputs,  $r_\phi(n) = C\sqrt{WL \log W \log n}/\sqrt{n}$ , where  $W$  is the total number of weights,  $L$  is the number of layers, and  $C$  is a constant independent of  $n$  and  $W$  [13, 51]. This rate is parametric but scales linearly with  $W$ , which is problematic for overparameterized networks. For 1-Lipschitz activations and bounded weights, [15] derive a rate of  $r_\phi(n) = C\sqrt{\prod_{l=1}^L M(l)}/n^{1/4}$ , where  $M(l)$  bounds the Frobenius norm of layer  $l$ 's weight matrix.

**Practical Guidance in High-Dimensional Settings** When  $\phi(x)$  is high-dimensional, managing the complexity of  $\mathcal{B}_\phi$  through regularization is critical since we are using the bias function  $b(x)$  to extrapolate the CATE beyond low-variance regions where compliance is low and overfitting risks are high. In the parametric extrapolation approach (Section 4.1), implementing  $L_1$  or  $L_2$  regularization via Lasso or Ridge regression in the final step effectively controls model complexity. In the shared representation approach in Example 1, regularization not only helps control the parameters  $h^O$  and  $\nu$ , but can also prevent over-parametrization in the neural network  $\phi$ . The choice between  $L_1$  and  $L_2$  regularization, and their application, should align with the data-generating process and the desired model characteristics.

## 5 Experimental Results

We apply our method to both simulated and real-world data. First, we use the confounded synthetic data example from [26], along with a similar DGP to simulate an IV study, maintaining the same confounding structure and treatment effects. Using this DGP, we evaluate Algorithm 1 and Algorithm 2 in estimating the unbiased CATE by integrating these datasets. Next, we demonstrate our estimators on a real-world dataset examining the impact of 401(k) participation on financial wealth. Details on model implementation, hyperparameter selection, and validation procedures are in Appendix C. The replication code is available at <https://github.com/CausalML/Weak-Instruments-Obs-Data-CATE>.

### 5.1 Simulation Studies

We generate the observational dataset  $O = (X^O, A^O, Y^O)$  as follows (see [26]):

$$\begin{aligned} X &\sim \mathcal{N}(0, 1), \quad A \sim \text{Bern}(0.5), \quad U \mid X, A \sim \mathcal{N}(X(A - 0.5), 0.75) \\ Y &= 1 + A + X + 2AX + 0.5X^2 + 0.75AX^2 + U + 0.5\epsilon_Y, \quad \epsilon_Y \sim \mathcal{N}(0, 1) \end{aligned} \quad (7)$$

In this DGP, the true CATE is given by  $\tau(x) = 0.75x^2 + 2x + 1$ , whereas the biased observational CATE is represented by  $\tau^O(x) = 0.75x^2 + x + 1$ . This results in a bias  $b(x) = x$ , which is linear in  $x$ . We modify this DGP to generate the experimental IV dataset  $E = (X^E, Z^E, A^E, Y^E)$  as follows:

$$\begin{aligned} X &\sim \mathcal{N}(0, 1), \quad Z \sim \text{Bern}(0.5), \quad A^* \sim \text{Bern}(0.5) \\ \gamma(X) &= \sigma(2X), \quad C \sim \text{Bern}(\gamma(X)), \quad A = C \cdot Z + (1 - C) \cdot A^* \\ U \mid X, A, C &\sim C \cdot \mathcal{N}(0, 1) + (1 - C) \cdot \mathcal{N}(X(A - 0.5), 0.75) \end{aligned}$$

where  $C$  is the (unknown) compliance indicator,  $\sigma$  is the logistic sigmoid and we keep the same outcome function as in Equation 7. In this modified DGP, the randomized instrument has compliance sharply determined by  $X$ , with low  $X$  values indicating almost no compliance and high  $X$  values indicating near-perfect compliance.

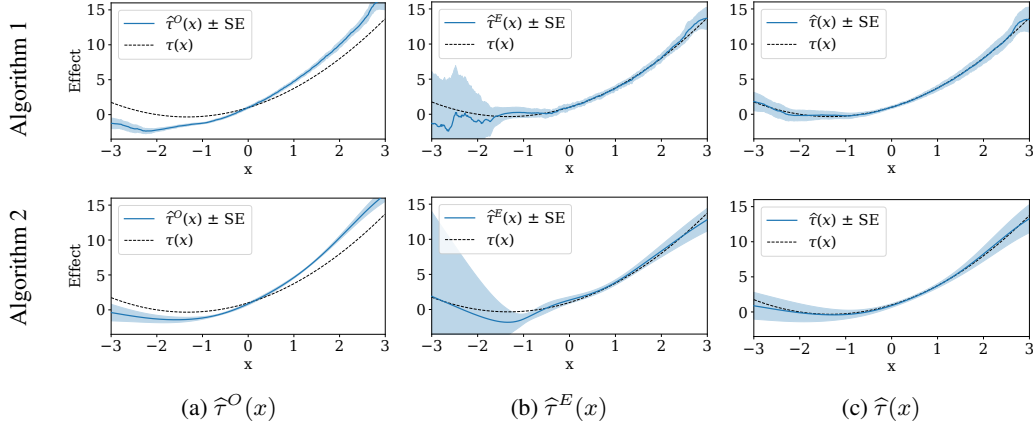


Figure 1: Means and standard errors of estimates from 100 simulated dataset pairs ( $O, E$ ) using Random Forest (top) or Neural Network (bottom) learners. (1a): Biased observational CATE  $\tau^O(x)$ . (1b): High variance CATEs from the IV dataset using Equation 3. (1c): CATEs from Algorithm 2 using parametric extrapolation (top) or representation learning (bottom).

We generate 100 observational and IV datasets, each with 5000 samples, from the proposed DGP. We apply Algorithm 1 to each dataset. With a randomized instrument,  $\pi_Z(x) = 0.5$ . We estimate  $\gamma(x)$  as the difference between Random Forest (RF) classifiers trained on  $X^E, A^E \mid Z^E = 0$  and  $X^E, A^E \mid Z^E = 1$ . The biased observational CATE is modeled using the T-learner approach [30], with RF regressors trained on  $X^O, Y^O \mid A^E = 0$  and  $X^O, Y^O \mid A^O = 1$ . For comparison, we implement a CATE estimator for the experimental data using Equation 3. We compute  $\delta_Y(x)$  as the difference between RF regressors trained on  $X^E, Y^E \mid Z^E = 0$  and  $X^E, Y^E \mid Z^E = 1$ , then divide by  $\hat{\gamma}(x)$ , clipping the compliance score at 0.1. We calculate  $\hat{\gamma}$ ,  $\hat{\tau}^O(x)$ , and  $\hat{\tau}^E(x)$  for each dataset pair and proceed with the second step of Algorithm 1 by setting  $\phi(x) = x$ .

In Figure 1 (top row), we show the means and standard errors of our estimators across 100 simulations. The first two plots illustrate the learned observational CATE  $\hat{\tau}^O(x)$  and the learned IV CATE  $\hat{\tau}^E(x)$ . As expected,  $\hat{\tau}^O(x)$  shows clear bias, while  $\hat{\tau}^E(x)$  has high variance despite aggressive compliance score clipping. The third plot presents results from Algorithm 1, showing that  $\hat{\tau}(x)$  is unbiased and has low variance across  $\mathcal{X}$ , effectively leveraging the strengths of both datasets to capture the true CATE and address the limitations of each individual study design.

We note that in our DGP,  $\tau(x)$ ,  $\tau^O(x)$ , and  $b(x)$  are linear in the polynomial representation  $(x, x^2)$ . Thus, we use Algorithm 2 with Example 1 to learn the true CATE and the common representation from the generated dataset. For consistency, we employ feed-forward neural networks (NNs) to estimate all quantities. The estimator for  $\hat{\gamma}$  uses a NN with a sigmoid activation in the output layer, trained on  $X^E$  with the pseudo-outcome  $2A^E Z^E - 2A^E(1 - Z^E)$ . The representation  $\phi(x)$  and the biased CATE  $\tau^O(x)$  are derived using a representation network with two output heads for learning  $Y^O \mid X^O, A^O = 0$  and  $Y^O \mid X^O, A^O = 1$ . A similar dual-head approach is used to learn  $\delta_Y(x)$ , focusing on  $Y^E \mid X^E, Z^E = 0$  and  $Y^E \mid X^E, Z^E = 1$ . When calculating  $\delta_Y(x)/\gamma(x)$ , we clip the compliance score at 0.1. Unlike Algorithm 1, we don't guarantee the polynomial representation will be fully captured by the chosen representation class, but we expect a sufficiently flexible  $\Phi$  to adequately represent these relationships.

The means and standard errors of our estimators from 100 simulations using neural networks and Algorithm 2 are shown in Figure 1 (bottom row). As before,  $\hat{\tau}^O(x)$  shows bias, while  $\hat{\tau}^E(x)$  has high variance in low-compliance regions, despite score clipping. However, Figure 1c shows that  $\hat{\tau}$  remains unbiased with relatively low variance across  $\mathcal{X}$ . This demonstrates that combining observational and IV data, where the biased and true CATE share a representation, allows us to reliably learn both the representation and the unbiased CATE, overcoming the limitations of each individual study.

## 5.2 Impact of 401(k) Participation on Financial Wealth

We demonstrate our method's effectiveness with a real-world case study on the impact of 401(k) participation on financial wealth, using data from the 1991 Survey of Income and Program Participation [9]. The dataset includes 9,915 respondents with nine covariates: age, income, education,



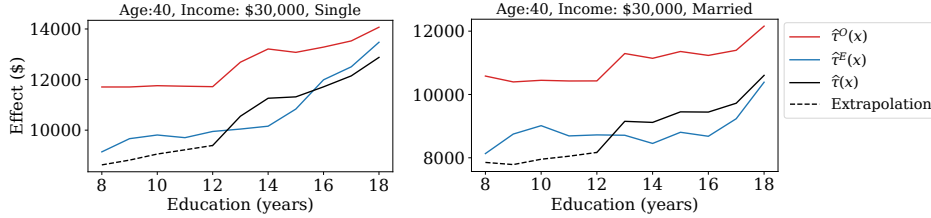


Figure 2: Impact of 401(k) participation on net worth by education level: Using  $\hat{\tau}$  from Algorithm 1, we fix age, income, and binary variables, varying education and marital status. The black line shows results from Algorithm 1, and the dashed line indicates predictions in the no-compliance region.  $\hat{\tau}^O$  is the observational CATE, while  $\hat{\tau}^E$  is the IV CATE without non-compliance.

family size, marital status, two-earner status, pension status, IRA participation, and home ownership. The primary variable of interest is 401(k) participation ( $A$ ), with eligibility ( $Z$ ) as the instrumental variable. Although 401(k) eligibility is not randomly assigned, it is argued to maintain conditional independence given observed features [9, 38]. We assume 401(k) eligibility influences net worth only through 401(k) participation, characterizing this as an IV study with one-sided non-compliance, where non-eligible individuals cannot participate. The target variable ( $Y$ ) is net financial assets, calculated as the total of 401(k) balance, bank account balances, and interest-earning assets, minus non-mortgage debt.

To replicate the scenario, we split the dataset into two halves: one for the IV study and the other for the observational study (where the instrument information is removed). Our goal is to use the parametric extension approach in Algorithm 1 to recover unbiased CATEs. Due to one-sided non-compliance, the estimated compliance factor  $\hat{\gamma}(x)$  is high (0.49 – 0.90, see Appendix C). We introduce non-compliance by setting  $\gamma(x)$  to 0 for individuals with less than 12 years of education (13% of the population). In the first stage of Algorithm 1, we use RF regressors and classifiers to estimate  $\tau^O(x)$ ,  $\gamma(x)$ , and  $\pi_Z(x)$ , with hyperparameters from [10]. In the second stage, we define the mapping  $\phi(x)$  with an intercept term, the 9 covariates, and their interactions (46 features total). We apply mild  $L_1$  regularization in the final linear regression due to the large number of features.

In Figure 2, we analyze how the CATE function from Algorithm 1 varies with education. We focus on education because compliance selects education as a top importance feature, whereas the outcome models do not (see Appendix C). We vary education and marital status, setting age and income to the median and binary variables to zero. Since compliance in the IV study is high, we consider  $\hat{\tau}^E$  without artificial non-compliance as the ground truth. We observe that observational data treatment effects are upwardly biased due to unobserved confounders (e.g., financial literacy). The  $\hat{\tau}(x)$  from Algorithm 1, shown with a dashed line for non-compliance regions, closely follows  $\hat{\tau}^E(x)$ . This demonstrates that combining IV and observational data effectively estimates unbiased CATEs in real-world scenarios, proving robust for causal inference with low compliance and unobserved confounding.

## 6 Conclusion

This study introduces a method that combines observational and instrumental variable (IV) data to tackle unobserved confounders in observational studies and low compliance in IV studies. Our two-stage framework first identifies biased CATEs from observational data, then corrects them using compliance-weighted IV samples. We explore two versions: one with a parametric form for confounding bias and another with a shared representation between true and biased CATE. We showed that both methods are consistent and validated through simulations and real-world applications. Our method is promising for applications in digital platforms, personalized medicine, and economics. This research represents an important advancement toward more reliable and actionable insights in complex data environments. Limitations of our work are discussed in Appendix D.

## References

- [1] A. Abadie, J. Gu, and S. Shen. Instrumental variable estimation with first-stage heterogeneity. *Journal of Econometrics*, 240(2):105425, 2024.
- [2] A. Agresti. *Foundations of linear and generalized linear models*. John Wiley & Sons, 2015.

- [3] I. Andrews, J. H. Stock, and L. Sun. Weak instruments in instrumental variables regression: Theory and practice. *Annual Review of Economics*, 11:727–753, 2019.
- [4] J. D. Angrist, G. W. Imbens, and D. B. Rubin. Identification of causal effects using instrumental variables. *Journal of the American statistical Association*, 91(434):444–455, 1996.
- [5] O. Atan, J. Jordon, and M. Van der Schaar. Deep-treat: Learning optimal personalized treatments from observational data using neural networks. In *Proceedings of the AAAI Conference on Artificial Intelligence*, volume 32, 2018.
- [6] S. Athey, R. Chetty, and G. Imbens. Combining experimental and observational data to estimate treatment effects on long term outcomes. *arXiv preprint arXiv:2006.09676*, 2020.
- [7] A. Bennett, N. Kallus, and T. Schnabel. Deep generalized method of moments for instrumental variable analysis. *Advances in neural information processing systems*, 32, 2019.
- [8] D. Cheng and T. Cai. Adaptive combination of randomized and observational data. *arXiv preprint arXiv:2111.15012*, 2021.
- [9] V. Chernozhukov and C. Hansen. The effects of 401 (k) participation on the wealth distribution: an instrumental quantile regression analysis. *Review of Economics and statistics*, 86(3):735–751, 2004.
- [10] V. Chernozhukov, D. Chetverikov, M. Demirer, E. Duflo, C. Hansen, W. Newey, and J. Robins. Double/debiased machine learning for treatment and structural parameters, 2018.
- [11] S. Coussens and J. Spiess. Improving inference from simple instruments through compliance estimation. *arXiv preprint arXiv:2108.03726*, 2021.
- [12] A. Curth, A. M. Alaa, and M. van der Schaar. Estimating structural target functions using machine learning and influence functions. *arXiv preprint arXiv:2008.06461*, 2020.
- [13] M. H. Farrell, T. Liang, and S. Misra. Deep neural networks for estimation and inference. *Econometrica*, 89(1):181–213, 2021.
- [14] D. J. Foster and V. Syrgkanis. Orthogonal statistical learning. *The Annals of Statistics*, 51(3): 879–908, 2023.
- [15] N. Golowich, A. Rakhlin, and O. Shamir. Size-independent sample complexity of neural networks. In *Conference On Learning Theory*, pages 297–299. PMLR, 2018.
- [16] Google. Google colab. <https://colab.research.google.com/>, 2024. Accessed: April 2024.
- [17] P. R. Hahn, J. S. Murray, and C. M. Carvalho. Bayesian regression tree models for causal inference: Regularization, confounding, and heterogeneous effects (with discussion). *Bayesian Analysis*, 15(3):965–1056, 2020.
- [18] J. Hartford, G. Lewis, K. Leyton-Brown, and M. Taddy. Deep iv: A flexible approach for counterfactual prediction. In *International Conference on Machine Learning*, pages 1414–1423. PMLR, 2017.
- [19] T. Hatt and S. Feuerriegel. Sequential deconfounding for causal inference with unobserved confounders. In *Causal Learning and Reasoning*, pages 934–956. PMLR, 2024.
- [20] T. Hatt, J. Berrevoets, A. Curth, S. Feuerriegel, and M. van der Schaar. Combining observational and randomized data for estimating heterogeneous treatment effects. *arXiv preprint arXiv:2202.12891*, 2022.
- [21] J. L. Hill. Bayesian nonparametric modeling for causal inference. *Journal of Computational and Graphical Statistics*, 20(1):217–240, 2011.
- [22] A. Huang, M. Chandra, and L. Malkhasyan. Weak instrumental variables: Limitations of traditional 2sls and exploring alternative instrumental variable estimators. *arXiv preprint arXiv:2104.12370*, 2021.

- [23] G. Imbens, N. Kallus, X. Mao, and Y. Wang. Long-term causal inference under persistent confounding via data combination. *arXiv preprint arXiv:2202.07234*, 2022.
- [24] F. Johansson, U. Shalit, and D. Sontag. Learning representations for counterfactual inference. In *International conference on machine learning*, pages 3020–3029. PMLR, 2016.
- [25] N. Kallus and A. Zhou. Confounding-robust policy improvement. *Advances in neural information processing systems*, 31, 2018.
- [26] N. Kallus, A. M. Puli, and U. Shalit. Removing hidden confounding by experimental grounding. *Advances in neural information processing systems*, 31, 2018.
- [27] H. Kang, A. Zhang, T. T. Cai, and D. S. Small. Instrumental variables estimation with some invalid instruments and its application to mendelian randomization. *Journal of the American statistical Association*, 111(513):132–144, 2016.
- [28] E. H. Kennedy. Towards optimal doubly robust estimation of heterogeneous causal effects. *Electronic Journal of Statistics*, 17(2):3008–3049, 2023.
- [29] E. H. Kennedy, S. Balakrishnan, and M. G’Sell. Sharp instruments for classifying compliers and generalizing causal effects. 2020.
- [30] S. R. Künzel, J. S. Sekhon, P. J. Bickel, and B. Yu. Metalearners for estimating heterogeneous treatment effects using machine learning. *Proceedings of the national academy of sciences*, 116(10):4156–4165, 2019.
- [31] Y. Lin, F. Windmeijer, X. Song, and Q. Fan. On the instrumental variable estimation with many weak and invalid instruments. *Journal of the Royal Statistical Society Series B: Statistical Methodology*, page qkae025, 2024.
- [32] S. M. Lundberg and S.-I. Lee. A unified approach to interpreting model predictions. *Advances in neural information processing systems*, 30, 2017.
- [33] X. Nie and S. Wager. Quasi-oracle estimation of heterogeneous treatment effects. *Biometrika*, 108(2):299–319, 2021.
- [34] M. Oprescu, V. Syrgkanis, and Z. S. Wu. Orthogonal random forest for causal inference. In *International Conference on Machine Learning*, pages 4932–4941. PMLR, 2019.
- [35] M. Oprescu, J. Dorn, M. Ghoummaid, A. Jesson, N. Kallus, and U. Shalit. B-learner: Quasi-oracle bounds on heterogeneous causal effects under hidden confounding. In *International Conference on Machine Learning*, pages 26599–26618. PMLR, 2023.
- [36] A. Paszke, S. Gross, F. Massa, A. Lerer, J. Bradbury, G. Chanan, T. Killeen, Z. Lin, N. Gimelshein, L. Antiga, A. Desmaison, A. Kopf, E. Yang, Z. DeVito, M. Raison, A. Tejani, S. Chilamkurthy, B. Steiner, L. Fang, J. Bai, and S. Chintala. Pytorch: An imperative style, high-performance deep learning library. *NeurIPS*, 2019.
- [37] F. Pedregosa, G. Varoquaux, A. Gramfort, V. Michel, B. Thirion, O. Grisel, M. Blondel, P. Prettenhofer, R. Weiss, V. Dubourg, J. Vanderplas, A. Passos, D. Cournapeau, M. Brucher, M. Perrot, and E. Duchesnay. Scikit-learn: Machine learning in Python. *Journal of Machine Learning Research*, 12:2825–2830, 2011.
- [38] J. M. Poterba and S. F. Venti. 401 (k) plans and tax-deferred saving. In *Studies in the Economics of Aging*, pages 105–142. University of Chicago Press, 1994.
- [39] P. Probst, M. N. Wright, and A.-L. Boulesteix. Hyperparameters and tuning strategies for random forest. *Wiley Interdisciplinary Reviews: data mining and knowledge discovery*, 9(3): e1301, 2019.
- [40] P. R. Rosenbaum, P. Rosenbaum, and Briskman. *Design of observational studies*, volume 10. Springer, 2010.
- [41] E. T. Rosenman, G. Basse, A. B. Owen, and M. Baiocchi. Combining observational and experimental datasets using shrinkage estimators. *Biometrics*, 79(4):2961–2973, 2023.

- [42] U. Shalit, F. D. Johansson, and D. Sontag. Estimating individual treatment effect: generalization bounds and algorithms. In *International conference on machine learning*, pages 3076–3085. PMLR, 2017.
- [43] C. Shi, D. Blei, and V. Veitch. Adapting neural networks for the estimation of treatment effects. *Advances in neural information processing systems*, 32, 2019.
- [44] R. Singh, M. Sahani, and A. Gretton. Kernel instrumental variable regression. *Advances in Neural Information Processing Systems*, 32, 2019.
- [45] V. Syrgkanis, V. Lei, M. Oprescu, M. Hei, K. Battocchi, and G. Lewis. Machine learning estimation of heterogeneous treatment effects with instruments. *Advances in Neural Information Processing Systems*, 32, 2019.
- [46] S. Wager and S. Athey. Estimation and inference of heterogeneous treatment effects using random forests. *Journal of the American Statistical Association*, 113(523):1228–1242, 2018.
- [47] L. Wang and E. Tchetgen Tchetgen. Bounded, efficient and multiply robust estimation of average treatment effects using instrumental variables. *Journal of the Royal Statistical Society Series B: Statistical Methodology*, 80(3):531–550, 2018.
- [48] Y. Wang and D. M. Blei. The blessings of multiple causes. *Journal of the American Statistical Association*, 114(528):1574–1596, 2019.
- [49] L. Xu, Y. Chen, S. Srinivasan, N. de Freitas, A. Doucet, and A. Gretton. Learning deep features in instrumental variable regression. *arXiv preprint arXiv:2010.07154*, 2020.
- [50] S. Yang and P. Ding. Combining multiple observational data sources to estimate causal effects. *Journal of the American Statistical Association*, 2019.
- [51] D. Yarotsky. Error bounds for approximations with deep relu networks. *Neural Networks*, 94: 103–114, 2017.

## A Extended Literature Review

**Heterogeneous treatment effect estimation from observational data** Recently, there has been a significant interest in applying machine learning to estimate CATEs using observational data. This field has seen adaptations of a wide range of machine learning techniques, from random forests [34, 46] and Bayesian algorithms *e.g.* [17, 21] to deep learning [5, 24, 43] and blackbox meta-learners [30, 33] that utilize efficient influence functions [12, 28] and Neyman orthogonality [10, 14]. Despite these advancements, a significant challenge persists as these methods typically assume the absence of confounding in observational data (ignorability) – an often unrealistic and unverifiable assumption – limiting their real-world applicability. Without ignorability, point identification of effects is impossible, although some studies propose methods to construct *bounds* on treatment effect estimates under assumptions about the structure of unobserved confounding [19, 25, 35, 40, 48]. Nonetheless, these bounds often have limited practical utility.

**Heterogeneous treatment effect estimation using IVs** Machine learning techniques have recently been integrated with instrumental variable methods, offering significant advantages over traditional approaches, including the flexible estimation of CATEs. [44] and [49] expand on two-stage least squares (2SLS) to incorporate complex feature mappings via kernel methods and deep learning. In the same vein, [18] introduced a two-stage neural network for conditional density estimation, while [7] applied moment conditions for IV estimation. [45] propose novel IV estimators that exhibit Neyman orthogonality. However, these techniques rely on the assumption that instruments are relevant across all covariate groups, a condition that is not consistently met with weak instruments.

**Treatment effect estimation with weak instruments** Weak instruments compromise the reliability of traditional IV methods like 2SLS, often producing biased, high-variance estimates and undermining causal claims. To mitigate these issues, several approaches have been developed, including bias-adjusted 2SLS estimators, limited information maximum likelihood (LIML), and jackknife instrumental variable (JIVE) estimators (see [22] and references therein). Recent methods reduce 2SLS estimator variance by exploiting first-stage heterogeneity (variation in compliance) through a weighting scheme, as detailed in [1, 11, 29]. However, these methods do not extend to estimating conditional average treatment effects. Another strand of research focuses on combining multiple weak instruments into a robust composite, showing promise in genetic studies using Mendelian randomization ([27, 31]). These approaches require access to multiple weak instruments for the same treatment. Our work aligns most closely with [1, 11, 29] in that we leverage compliance heterogeneity and employ compliance weighting to merge IV studies with observational data for efficient confounding bias estimation. Unlike these studies, however, our approach distinctively estimates heterogeneous effects and leverages additional observational data to address challenges posed by weak instruments.

**Combining observational and randomized data** There has been an proliferation of research in combining observational datasets with randomized control trials (RCT) – experimental data with *perfect* compliance – to mitigate bias from observational studies. One of the strategies is to impose structural assumptions such as strong parametric assumptions for the confounding bias [26] or a shared structure between the biased and unbiased CATE functions that can be estimated from the two datasets [20]. Other studies advocate for dual estimators from both data types, optimizing bias correction through a weighted average [8, 41, 50]. Additionally, approaches like those by [6] and [23] leverage outcomes from different time-steps, such as short-term and long-term effects, to enhance estimation accuracy. Our work is closest to [26] and [20]. However, our study faces additional complexities: firstly, the CATE estimation techniques differ between the datasets, requiring us to debias the overall effect function rather than just individual outcome functions. Secondly, while randomized control trials (RCTs) may not represent the target population due to their narrow scope, our instrumental variable (IV) study faces representation issues due to minimal or absent compliance in strata that are not known a priori. Thirdly, the CATE estimation in our IV study uses a ratio estimator, which is highly sensitive to changes in the compliance denominator, adding a layer of complexity to our analysis.

## B Proofs of Theorems and Lemmas

### B.1 Proof of Lemma 1

Recall that for any  $x \in \mathcal{X}'$ , we have that  $\gamma(x) > 0$  by Assumption 2. Then, assuming that  $\pi_Z(x) > 0$ , we use the law of total expectation as follows:

$$\begin{aligned}
& \mathbb{E} \left[ \frac{Y^E Z^E}{\pi_Z(x)\gamma(x)} - \frac{Y^E(1-Z^E)}{(1-\pi_Z(x))\gamma(x)} \middle| X^E = x \right] \\
&= \mathbb{E} \left[ \frac{Y^E Z^E}{\pi_Z(x)\gamma(x)} - \frac{Y^E(1-Z^E)}{(1-\pi_Z(x))\gamma(x)} \middle| Z^E = 1, X^E = x \right] P(Z^E = 1 | X^E = x) \\
&\quad + \mathbb{E} \left[ \frac{Y^E Z^E}{\pi_Z(x)\gamma(x)} - \frac{Y^E(1-Z^E)}{(1-\pi_Z(x))\gamma(x)} \middle| Z^E = 0, X^E = x \right] P(Z^E = 0 | X^E = x) \\
&= \mathbb{E} \left[ \frac{Y^E}{\pi_Z(x)\gamma(x)} \middle| Z^E = 1, X^E = x \right] \pi_Z(x) \\
&\quad - \mathbb{E} \left[ \frac{Y^E}{(1-\pi_Z(x))\gamma(x)} \middle| Z^E = 0, X^E = x \right] (1-\pi_Z(x)) \\
&= \frac{\mathbb{E}[Y^E | Z^E = 1, X^E = x] - \mathbb{E}[Y^E | Z^E = 0, X^E = x]}{\gamma(x)} \\
&= \frac{\mathbb{E}[A^E | Z^E = 1, X^E = x] - \mathbb{E}[A^E | Z^E = 0, X^E = x]}{\mathbb{E}[A^E | Z^E = 1, X^E = x] - \mathbb{E}[A^E | Z^E = 0, X^E = x]} = \tau(x) \tag{Equation 3}
\end{aligned}$$

where the intermediate steps follow from the definitions of  $\pi_Z(x)$  and  $\gamma(x)$  and the last equality comes from the identification result in Equation 3.

### B.2 Proof of Theorem 2

For simplicity, we omit the  $E$  subscripts from  $X^E, Z^E, A^E, Y^E$  throughout this proof. Furthermore, assume that  $n_E$  is an integer multiple of the number of folds  $K$ . Let  $\widehat{\mathbb{E}}_k f(Z) = \frac{1}{|\mathcal{I}_k|} \sum_{i \in \mathcal{I}_k} f(Z_i)$ , recalling that  $\mathcal{I}_k = \{i \in \{1, \dots, n_E\} : i = k - 1 \pmod{K}\}$ , which indexes the subset of data in the  $k^{\text{th}}$  fold. Then, we can write the estimated parameter  $\widehat{\theta}$  as:

$$\begin{aligned}
\widehat{\theta} &= \left( \frac{1}{K} \sum_{k=1}^K \widehat{\mathbb{E}}_k \left[ \widehat{w}^{(k)}(X)^2 \phi(X) \phi(X)^T \right] \right)^{-1} \\
&\quad \cdot \frac{1}{K} \sum_{k=1}^K \widehat{\mathbb{E}}_k \left[ \left( YZ(1 - \widehat{\pi}_Z^{(k)}(X)) - Y(1-Z)\widehat{\pi}_Z^{(k)}(X) - \widehat{w}^{(k)}(X)\widehat{\tau}^O(X) \right) \widehat{w}^{(k)}(X)\phi(X) \right]
\end{aligned}$$

We also define the following quantities:

$$\begin{aligned}
\widetilde{\theta}_{n_E} &= \widehat{\mathbb{E}}_{n_E} \left[ w(X)^2 \phi(X) \phi(X)^T \right]^{-1} \\
&\quad \cdot \widehat{\mathbb{E}}_{n_E} \left[ (YZ(1 - \pi_Z(X)) - Y(1-Z)\pi_Z(X) - w(X)\tau^O(X)) w(X)\phi(X) \right] \\
\widetilde{\theta} &= \mathbb{E} \left[ w(X)^2 \phi(X) \phi(X)^T \right]^{-1} \\
&\quad \cdot \mathbb{E} \left[ (YZ(1 - \pi_Z(X)) - Y(1-Z)\pi_Z(X) - w(X)\tau^O(X)) w(X)\phi(X) \right]
\end{aligned}$$

We note that these quantities are well defined because  $\mathbb{E} \left[ w(X)^2 \phi(X) \phi(X)^T \right]$  is invertible. This is derived from the first and last conditions of Assumption 3, along with the stipulation in Assumption 1 that  $\gamma(x) > 0$  for all  $x$  in a set of non-zero measure. Using these definitions, we can write

$$\begin{aligned}
\|\widehat{\theta} - \theta\|_2 &= \left\| \widehat{\theta} - \widetilde{\theta}_{n_E} + \widetilde{\theta}_{n_E} - \widetilde{\theta} + \widetilde{\theta} - \theta \right\|_2 \\
&\leq \underbrace{\|\widehat{\theta} - \widetilde{\theta}_{n_E}\|_2}_{\lambda_1} + \underbrace{\|\widetilde{\theta}_{n_E} - \widetilde{\theta}\|_2}_{\lambda_2} + \underbrace{\|\widetilde{\theta} - \theta\|_2}_{\lambda_3} \tag{Cauchy-Schwartz}
\end{aligned}$$

We study these terms separately. We notice that  $\lambda_2$  is just linear regression of the modified outcome  $YZ(1 - \pi_Z(X)) - Y(1 - Z)\pi_Z(X) - w(X)\tau^O(X)$  on  $\phi(X)$  using weights  $w(X)$ . Given the regularity conditions in Assumption 3 (which subsume the standard regularity conditions of linear regression), we have that  $\lambda_2$  is  $O_p(1/\sqrt{n_E})$ . Then, consider the  $\theta$  term. We have:

$$\begin{aligned}
\tilde{\theta} &= \mathbb{E} [w(X)^2 \phi(X) \phi(X)^T]^{-1} \\
&\quad \cdot \mathbb{E} [(YZ(1 - \pi_Z(X)) - Y(1 - Z)\pi_Z(X) - w(X)\tau^O(X)) w(X) \phi(X)] \\
&= \mathbb{E} [w(X)^2 \phi(X) \phi(X)^T]^{-1} \\
&\quad \cdot \mathbb{E} [(YZ(1 - \pi_Z(X)) - Y(1 - Z)\pi_Z(X) + w(X)\tau(X) - w(X)\theta^T \phi(X)) w(X) \phi(X)] \\
&\hspace{15em} \text{(Realizability of } b(X)\text{)} \\
&= \mathbb{E} [w(X)^2 \phi(X) \phi(X)^T \mid \gamma(X) > 0]^{-1} P(\gamma(X) > 0)^{-1} \\
&\quad \cdot \left( \mathbb{E} [(YZ(1 - \pi_Z(X)) - Y(1 - Z)\pi_Z(X) - w(X)\tau(X)) w(X) \phi(X) \mid \gamma(X) > 0] \right. \\
&\quad \left. + \mathbb{E} [w(X)^2 \phi(X) \phi(X)^T \theta \mid \gamma(X) > 0] \right) P(\gamma(X) > 0) \\
&= \mathbb{E} [w(X)^2 \phi(X) \phi(X)^T \mid \gamma(X) > 0]^{-1} \\
&\quad \cdot \mathbb{E} [(YZ(1 - \pi_Z(X)) - Y(1 - Z)\pi_Z(X) - w(X)\tau(X)) w(X) \phi(X) \mid \gamma(X) > 0] + \theta \\
&= \mathbb{E} [w(X)^2 \phi(X) \phi(X)^T \mid \gamma(X) > 0]^{-1} \\
&\quad \cdot \mathbb{E} \left[ \left( \frac{YZ}{\pi_Z(X)\gamma(X)} - \frac{Y(1 - Z)}{(1 - \pi_Z(X))\gamma(X)} - \tau(X) \right) w^2(X) \phi(X) \mid \gamma(X) > 0 \right] + \theta \\
&\hspace{15em} \text{(Since } \gamma(X) > 0 \text{ implies } w(X) > 0 \text{ by Assumption 3)} \\
&= \theta. \hspace{15em} \text{(Lemma 1)}
\end{aligned}$$

Thus,  $\tilde{\theta} = \theta$  which implies  $\lambda_3 = 0$ . We now tackle the  $\lambda_1$  term. To streamline the exposition, let us introduce the following shorthand notation:

$$\begin{aligned}
\widehat{Y}^{(k)} &:= YZ(1 - \widehat{\pi}_Z^{(k)}(X)) - Y(1 - Z)\widehat{\pi}_Z^{(k)}(X) \\
\widetilde{Y} &:= YZ(1 - \pi_Z(X)) - Y(1 - Z)\pi_Z(X) \\
\widehat{\Sigma}_K &:= \frac{1}{K} \sum_{k=1}^K \widehat{\mathbb{E}}_k [ \widehat{w}^{(k)}(X)^2 \phi(X) \phi(X)^T ] \\
\Sigma_K &:= \mathbb{E} [ \widehat{w}^{(k)}(X)^2 \phi(X) \phi(X)^T ] \\
\widehat{\Sigma} &:= \widehat{\mathbb{E}}_{n_E} [ w(X)^2 \phi(X) \phi(X)^T ] \\
\Sigma &:= \mathbb{E} [ w(X)^2 \phi(X) \phi(X)^T ]
\end{aligned}$$

We can then write the  $\widehat{\theta} - \widetilde{\theta}_{n_E}$  as follows:

$$\begin{aligned}
&\widehat{\theta} - \widetilde{\theta}_{n_E} \\
&= \widehat{\Sigma}_K^{-1} \frac{1}{K} \sum_{k=1}^K \widehat{\mathbb{E}}_k \left[ \left( \widehat{Y}^{(k)} - \widehat{w}^{(k)}(X) \widehat{\tau}^O(X) \right) \widehat{w}^{(k)}(X) \phi(X) \right] \\
&\quad - \widehat{\Sigma}^{-1} \widehat{\mathbb{E}}_{n_E} \left[ \left( \widetilde{Y} - w(X) \tau^O(X) \right) w(X) \phi(X) \right] \\
&= \left( \widehat{\Sigma}_K^{-1} - \widehat{\Sigma}^{-1} \right) \frac{1}{K} \sum_{k=1}^K \widehat{\mathbb{E}}_k \left[ \left( \widehat{Y}^{(k)} - \widehat{w}^{(k)}(X) \widehat{\tau}^O(X) \right) \widehat{w}^{(k)}(X) \phi(X) \right] \tag{\lambda_{1,1}}
\end{aligned}$$

$$\begin{aligned}
&+ \widehat{\Sigma}^{-1} \frac{1}{K} \sum_{k=1}^K \left( \mathbb{E} [ \left( \widehat{Y}^{(k)} - \widehat{w}^{(k)}(X) \widehat{\tau}^O(X) \right) \widehat{w}^{(k)}(X) \phi(X) ] \right. \\
&\quad \left. - \mathbb{E} [ \left( \widetilde{Y} - w(X) \tau^O(X) \right) w(X) \phi(X) ] \right) \tag{\lambda_{1,2}}
\end{aligned}$$

$$\begin{aligned}
& + \widehat{\Sigma}^{-1} \frac{1}{K} \sum_{k=1}^K (\widehat{\mathbb{E}}_k - \mathbb{E}) \left[ \left( \widehat{Y}^{(k)} - \widehat{w}^{(k)}(X) \widehat{\tau}^O(X) \right) \widehat{w}^{(k)}(X) \phi(X) \right. \\
& \quad \left. - \left( \widetilde{Y} - w(X) \tau^O(X) \right) w(X) \phi(X) \right] \tag{\lambda_{1,3}}
\end{aligned}$$

By Cauchy-Schwartz, we can bound the  $\lambda_1$  term as

$$\lambda_1 = \left\| \widehat{\theta} - \widetilde{\theta}_{n_E} \right\|_2 \leq \sum_{i=1}^3 \|\lambda_{1,i}\|_2,$$

where we used the  $\lambda_{1,i}$  notation introduced in the preceding equation. We bound each of the  $\lambda_{1,i}$ 's separately. We let  $\|A\|_F$  denote the Frobenius norm of the matrix  $A$ . Then, consider  $\lambda_{1,1}$ :

$$\begin{aligned}
& \|\lambda_{1,1}\|_2 \\
& \leq \left\| \widehat{\Sigma}_K^{-1} - \widehat{\Sigma}^{-1} \right\|_F \left\| \frac{1}{K} \sum_{k=1}^K \widehat{\mathbb{E}}_k \left[ \left( \widehat{Y}^{(k)} - \widehat{w}^{(k)}(X) \widehat{\tau}^O(X) \right) \widehat{w}^{(k)}(X) \phi(X) \right] \right\|_2 \\
& \quad \text{(Cauchy-Schwartz)} \\
& = \left\| \widehat{\Sigma}_K^{-1} (\widehat{\Sigma} - \widehat{\Sigma}_K) \widehat{\Sigma}^{-1} \right\|_F \left\| \frac{1}{K} \sum_{k=1}^K \widehat{\mathbb{E}}_k \left[ \left( \widehat{Y}^{(k)} - \widehat{w}^{(k)}(X) \widehat{\tau}^O(X) \right) \widehat{w}^{(k)}(X) \phi(X) \right] \right\|_2 \\
& \leq \left\| \widehat{\Sigma}_K^{-1} \right\|_F \left\| \widehat{\Sigma} - \widehat{\Sigma}_K \right\|_F \left\| \widehat{\Sigma}^{-1} \right\|_F \left\| \frac{1}{K} \sum_{k=1}^K \widehat{\mathbb{E}}_k \left[ \left( \widehat{Y}^{(k)} - \widehat{w}^{(k)}(X) \widehat{\tau}^O(X) \right) \widehat{w}^{(k)}(X) \phi(X) \right] \right\|_2 \\
& = O_p \left( \left\| \widehat{\Sigma} - \widehat{\Sigma}_K \right\|_F \right) \quad \text{(By the boundedness conditions in Assumption 3)}
\end{aligned}$$

Furthermore,

$$\begin{aligned}
\widehat{\Sigma} - \widehat{\Sigma}_K & = \widehat{\mathbb{E}}_{n_E} \left[ w(X)^2 \phi(X) \phi(X)^T \right] - \frac{1}{K} \sum_{k=1}^K \widehat{\mathbb{E}}_k \left[ \widehat{w}^{(k)}(X)^2 \phi(X) \phi(X)^T \right] \\
& = \frac{1}{K} \sum_{k=1}^K (\widehat{\mathbb{E}}_k - \mathbb{E}) \left[ \left( w(X)^2 - \widehat{w}^{(k)}(X)^2 \right) \phi(X) \phi(X)^T \right] \\
& \quad + \mathbb{E} \left[ \left( w(X)^2 - \widehat{w}^{(k)}(X)^2 \right) \phi(X) \phi(X)^T \right] \\
\Rightarrow \left\| \widehat{\Sigma} - \widehat{\Sigma}_K \right\|_F & \leq \frac{1}{K} \sum_{k=1}^K \left\| (\widehat{\mathbb{E}}_k - \mathbb{E}) \left[ \left( w(X)^2 - \widehat{w}^{(k)}(X)^2 \right) \phi(X) \phi(X)^T \right] \right\|_F \\
& \quad + \left\| \mathbb{E} \left[ \left( w(X)^2 - \widehat{w}^{(k)}(X)^2 \right) \phi(X) \phi(X)^T \right] \right\|_F \\
& \leq \frac{1}{K} \sum_{k=1}^K \sum_{i,j=1}^d \underbrace{\left| (\widehat{\mathbb{E}}_k - \mathbb{E}) \left[ \left( w(X)^2 - \widehat{w}^{(k)}(X)^2 \right) \phi(X)_i \phi(X)_j \right] \right|}_{:=\delta_k} \\
& \quad + \|w - \widehat{w}^k\|_{L_2} \mathbb{E} \left[ \left( w(X) + \widehat{w}^{(k)}(X) \right)^2 \left\| \phi(X) \phi(X)^T \right\|_F^2 \right]^{1/2} \\
& \quad \text{(Holder's inequality)}
\end{aligned}$$

By our boundedness assumptions, the second term yields an  $O_p(\|w - \widehat{w}^k\|_{L_2}) = O_p(r_\gamma(n_E) + r_{\pi_Z}(n_E))$  term in the expression for  $O_p(\|\widehat{\Sigma} - \widehat{\Sigma}_K\|_F)$ . To analyze the first term, let  $E_k$  represent the samples in the  $k^{\text{th}}$  fold of the  $E$  dataset. Then,  $\delta_k \mid E_k$  has mean 0 since  $\widehat{w}^{(k)}$  is independent from  $E_k$  due to the  $K$ -fold sample splitting. Then, we can apply Chebyshev's inequality to obtain that

$$\delta_k \mid E_k = O_p \left( n_E^{-1/2} \mathbb{E} \left[ \left( w(X)^2 - \widehat{w}^{(k)}(X)^2 \right)^2 \phi(X)_i^2 \phi(X)_j^2 \mid E_k \right] \right) = o_p(1/\sqrt{n_E})$$



from the consistency assumptions for  $\hat{\gamma}^{(k)}, \hat{\pi}_Z^{(k)}$  which translate into a consistency assumption for  $\hat{w}^{(k)}$ . By the bounded convergence theorem, this implies that  $\delta_k$  is also  $o_p(1/\sqrt{n_E})$ . Putting everything together, we obtain

$$\|\lambda_{1,1}\|_2 = O_p(r_\gamma(n_E) + r_{\pi_Z}(n_E)) + o_p(1/\sqrt{n_E}).$$

We now tackle  $\lambda_{1,2}$ :

$$\begin{aligned} & \lambda_{1,2} \\ &= \hat{\Sigma}^{-1} \frac{1}{K} \sum_{k=1}^K \left( \mathbb{E}[(\hat{Y}^{(k)} - \hat{w}^{(k)}(X)\hat{\tau}^O(X))\hat{w}^{(k)}(X)\phi(X)] \right. \\ & \quad \left. - \mathbb{E}[(\tilde{Y} - w(X)\tau^O(X))w(X)\phi(X)] \right) \\ & \|\lambda_{1,2}\|_2 \\ & \leq \|\hat{\Sigma}^{-1}\|_F \frac{1}{K} \sum_{k=1}^K \\ & \quad \cdot \sum_{i=1}^d \left| \mathbb{E} \left[ \left( \hat{w}^{(k)}(X)\hat{Y}^{(k)} - w(X)\tilde{Y} - \hat{w}^{(k)}(X)^2\hat{\tau}^O(X) + w(X)^2\tau^O(X) \right) \phi(X)_i \right] \right| \\ & \leq \|\hat{\Sigma}^{-1}\|_F \frac{1}{K} \\ & \quad \cdot \sum_{k=1}^K \sum_{i=1}^d \left\| \mathbb{E} \left[ \hat{w}^{(k)}(X)\hat{Y}^{(k)} - w(X)\tilde{Y} - \hat{w}^{(k)}(X)^2\hat{\tau}^O(X) + w(X)^2\tau^O(X) | X \right] \right\|_{L_2} \|\phi(X)_i\|_{L_2} \end{aligned}$$

Since the  $\|\phi(X)_i\|$ 's are bounded by assumption and  $\hat{\Sigma}^{-1} \xrightarrow{P} \Sigma^{-1}$  from the continuous mapping theorem, it suffices to study the term  $\mathbb{E} \left[ \hat{w}^{(k)}\hat{Y}^{(k)} - w(X)\tilde{Y} - \hat{w}^{(k)}(X)^2\hat{\tau}^O(X) + w(X)^2\tau^O(X) | X \right]$ :

$$\begin{aligned} & \left\| \mathbb{E} \left[ \hat{w}^{(k)}(X)\hat{Y}^{(k)} - w(X)\tilde{Y} - \hat{w}^{(k)}(X)^2\hat{\tau}^O(X) + w(X)^2\tau^O(X) | X \right] \right\|_{L_2} \\ & \leq \|\mathbb{E}[Y | Z = 1, X]\pi_Z(X)\{\hat{w}^{(k)}(X)(1 - \hat{\pi}_Z^{(k)}(x)) - w(X)(1 - \pi_Z(X))\}\|_{L_2} \\ & \quad + \|\mathbb{E}[Y | Z = 0, X](1 - \pi_Z(X))\{\hat{w}^{(k)}(X)\hat{\pi}_Z^{(k)}(x) - w(X)\pi_Z(X)\}\|_{L_2} \\ & \quad + \|\hat{w}^{(k)}(X)^2\hat{\tau}^O(X) - w(X)^2\tau^O(X)\|_{L_2} \\ & \lesssim \|\hat{w}^{(k)} - w\|_{L_2} + \|\hat{\gamma}^{(k)} - \gamma\|_{L_2} + \|\hat{\pi}_Z^{(k)} - \pi_Z\|_{L_2} + \|\hat{\tau}^O - \tau^O\|_{L_2} \\ & \hspace{15em} \text{(Boundedness assumptions)} \\ & \lesssim \|\hat{\gamma}^{(k)} - \gamma\|_{L_2} + \|\hat{\pi}_Z^{(k)} - \pi_Z\|_{L_2} + \|\hat{\tau}^O - \tau^O\|_{L_2} \\ & \hspace{15em} \text{(Definition of } w(X)\text{)} \\ & \leq r_\gamma(n_E) + r_{\pi_Z}(n_E) + r_{\tau^O}(n_O) \end{aligned}$$

where  $\lesssim$  absorbs constants. Thus,  $\|\lambda_{1,2}\|_2$  is  $O_p(r_\gamma(n_E) + r_{\pi_Z}(n_E) + r_{\tau^O}(n_O))$ . Lastly, we note that  $\lambda_{1,3}$  is the empirical process equivalent of  $\lambda_{1,2}$  and thus, by leveraging sample splitting through arguments similar those used for the  $\lambda_{1,1}$  term, we have that  $\|\lambda_{1,3}\|_2$  is  $o_p(1/\sqrt{n_E})$ . Putting all  $\lambda_{1,i}$  terms together, we have that  $\lambda_1$  is  $O_p(r_\gamma(n_E) + r_{\pi_Z}(n_E) + r_{\tau^O}(n_O)) + o_p(\sqrt{n_E})$ . Recall that  $\lambda_2$  is  $O_p(1/\sqrt{n_E})$  and  $\lambda_3 = 0$ , we obtain the desired result:

$$\|\hat{\theta} - \theta\|_2 = O_p(r_\gamma(n_E) + r_{\pi_Z}(n_E) + r_{\tau^O}(n_O) + 1/\sqrt{n_E}).$$

Given that  $\|\hat{\tau} - \tau\|_{L_2} = \|(\theta - \hat{\theta})^T \phi(X) + (\tau^O(X) - \tau^O(X))\|_{L_2}$ , we further have

$$\|\hat{\tau} - \tau\|_{L_2} = O_p(r_\gamma(n_E) + r_{\pi_Z}(n_E) + r_{\tau^O}(n_O) + 1/\sqrt{n_E})$$

by using the derived  $\hat{\theta}$  rates, the Cauchy-Schwartz inequality and the boundedness of  $\|\phi(X)\|_2$  assumption. Our proof is now complete.

### B.3 Proof of Theorem 3

We first study the convergence rate of  $\hat{\tau}^O$  using the conditions of Theorem 3. Assume that  $h^O$  and  $\phi(x)$  solve the following joint optimization problem:

$$\hat{h}^O, \hat{\phi} = \arg \min_{h^O \in \mathbb{R}^d, \phi \in \Phi} \sum_{i=1}^{n_O} \left( \left( \frac{Y^O A^O}{\hat{\pi}_A(X)} - \frac{Y^O(1-A^O)}{1-\hat{\pi}_A(X)} \right) - (h^O)^T \phi(X^O) \right)^2$$

Then,  $\hat{\tau}^O(x) = (\hat{h}^O)^T \hat{\phi}(x)$ . Thus, we write:

$$\begin{aligned} \|\tau^O - \hat{\tau}^O\|_{L_2} &\leq \|(h^O)^T \phi(X) - (\hat{h}^O)^T \hat{\phi}(X)\|_{L_2} \\ &\leq \|(h^O)^T \phi(X) - (\hat{h}^O)^T \phi(X)\|_{L_2} + \|(\hat{h}^O)^T (\phi(X) - \hat{\phi}(X))\|_{L_2} \\ &\lesssim \|h^O - \hat{h}^O\|_2 + r_\phi(n_O) \quad (\text{Boundedness assumptions}) \end{aligned}$$

We further expand the first term:

$$\begin{aligned} \|h^O - \hat{h}^O\|_2 &= \left\| \mathbb{E}[\phi(X)\phi(X)]^{-1} \mathbb{E}[\tilde{Y}\phi(X)] - \hat{\mathbb{E}}_{n_O}[\hat{\phi}(X)\hat{\phi}(X)]^{-1} \hat{\mathbb{E}}_{n_O}[\tilde{Y}\hat{\phi}(X)] \right\|_2 \\ &\quad \left( \tilde{Y} := \frac{Y^O A^O}{\hat{\pi}_A(X)} - \frac{Y^O(1-A^O)}{1-\hat{\pi}_A(X)} \right) \\ &\leq \left\| \mathbb{E}[\phi(X)\phi(X)]^{-1} \mathbb{E}[\tilde{Y}\phi(X)] - \mathbb{E}[\hat{\phi}(X)\hat{\phi}(X)]^{-1} \mathbb{E}[\tilde{Y}\hat{\phi}(X)] \right\|_2 \\ &\quad + \left\| \mathbb{E}[\hat{\phi}(X)\hat{\phi}(X)]^{-1} \mathbb{E}[\tilde{Y}\hat{\phi}(X)] - \hat{\mathbb{E}}_{n_O}[\hat{\phi}(X)\hat{\phi}(X)]^{-1} \hat{\mathbb{E}}_{n_O}[\tilde{Y}\hat{\phi}(X)] \right\|_2 \\ &= O_p(r_\phi(n_O) + 1/\sqrt{n_O}) \end{aligned}$$

Thus,  $\|\tau^O - \hat{\tau}^O\|_{L_2}$  is  $O_p(r_\phi(n_O) + 1/\sqrt{n_O})$ . Next, we build upon the insights provided by the Proof of Theorem 2. We note that we can apply the same analysis as in the Proof of Theorem 2 by using  $\hat{\phi}$  instead of  $\phi$  and everything goes through except the  $\lambda_3$  term which is not 0 since  $\nu$  depends on  $\phi$  and not  $\hat{\phi}$ . Thus, the convergence rate of  $\|\hat{\nu} - \nu\|_2$  will be  $O_p(r_\gamma(n_E) + r_{\pi_Z}(n_E) + r_{\tau^O}(n_O) + 1/\sqrt{n_E}) = O_p(r_\gamma(n_E) + r_{\pi_Z}(n_E) + r_\phi(n_O) + 1/\sqrt{n_E} + 1/\sqrt{n_O})$  plus a term that depends on the deviation between  $\hat{\phi}$  and  $\phi$ . This term is given by:

$$\begin{aligned} \lambda_3 &= \left\| \mathbb{E} \left[ w(X)^2 \hat{\phi}(X) \hat{\phi}(X)^T \right]^{-1} \right. \\ &\quad \cdot \mathbb{E} \left[ (YZ(1-\pi_Z(X)) - Y(1-Z)\pi_Z(X) - w(X)\tau^O(X)) w(X) \hat{\phi}(X) \right] - \nu \Big\|_2 \\ &= \left\| \mathbb{E} \left[ w(X)^2 \hat{\phi}(X) \hat{\phi}(X)^T \Big| \gamma(X) > 0 \right]^{-1} \mathbb{E} \left[ w(X)^2 \hat{\phi}(X) \phi(X)^T \nu \Big| \gamma(X) > 0 \right] - \nu \right\|_2 \\ &\quad (\text{Lemma 1}) \\ &= \left\| \mathbb{E} \left[ w(X)^2 \hat{\phi}(X) \hat{\phi}(X)^T \Big| \gamma(X) > 0 \right]^{-1} \mathbb{E} \left[ w(X)^2 \hat{\phi}(X) (\phi(X) - \hat{\phi}(X))^T \nu \Big| \gamma(X) > 0 \right] \right\|_2 \\ &= O_p(r_\phi(n_O)) \end{aligned}$$

However, this term simply gets absorbed into  $O_p(r_\gamma(n_E) + r_{\pi_Z}(n_E) + r_\phi(n_O) + 1/\sqrt{n_E} + 1/\sqrt{n_O})$ . Thus, we obtain the desired results:

$$\|\hat{\nu} - \nu\|_2 = O_p(r_\gamma(n_E) + r_{\pi_Z}(n_E) + r_\phi(n_O) + 1/\sqrt{n_E} + 1/\sqrt{n_O}),$$

and

$$\|\hat{\tau} - \tau\|_{L_2} = O_p(r_\gamma(n_E) + r_{\pi_Z}(n_E) + r_\phi(n_O) + 1/\sqrt{n_E} + 1/\sqrt{n_O}).$$

## C Additional Experimental Details

### C.1 Simulation Studies

The results for the parametric extension from Section 5.1 were generated on a consumer laptop equipped with a 13th Gen Intel Core i7 CPU. The execution took roughly 1.5 minutes using 20

Table 1: Hyperparameters of models in simulated data experiments.

Method	Model(s)	Algorithm	Hyperparameter	Value
Algorithm 1	Compliance	Random Forest ( <code>scikit-learn</code> )	max_depth	3
			min_samples_leaf	50
Algorithm 1	Outcomes	Random Forest ( <code>scikit-learn</code> )	max_depth	5
			min_samples_leaf	5
Algorithm 2	Representation CATE Compliance	Neural Network ( <code>PyTorch</code> )	activation	ELU
			hidden units	2
			network depth	5
			weight_decay	0.02
			optimizer	Adam
			learning rate	0.01
			batch size	2000
epochs	1000			

Table 2: 401(k) dataset description.

Name	Description	Type
age	age	continuous covariate
inc	income	continuous covariate
educ	years of completed education	continuous covariate
fsize	family size	continuous covariate covariate
marr	marital status	binary covariate
two_earn	whether dual-earning household	binary covariate
db	defined benefit pension status	binary covariate
pira	IRA participation	binary covariate
hown	home ownership	binary covariate
e401	401 (k) eligibility	binary instrument
p401	401 (k) participation	binary treatment
net_tfa	net financial assets	continuous outcome

concurrent workers. In contrast, the representation learning outcomes were derived using an NVIDIA Tesla T4 GPU on Google Colab [16]. The execution took approximately 1.5 hours, with half the time spent on Algorithm 2 and the other half on learning  $\hat{\tau}^E(x)$  over 100 iterations.

The Random Forest (RF) models used in Algorithm 1 employ the `RandomForestRegressor` and `RandomForestClassifier` algorithms from `scikit-learn` [37]. For the feed-forward neural networks within the representation learning component, we utilize the `nn` module from the `PyTorch` package [36]. Details regarding the hyperparameters for these models are provided in Table 1.

We configured the parameters for the Random Forest (RF) models based on theoretical guidance outlined by [39]. For the neural networks, we implemented early stopping using a validation dataset that constitutes 20% of the total generated datasets.

## C.2 Impact of 401(k) Participation on Financial Wealth

The dataset from [9] is comprised 9,915 observations with 9 covariates: age, income, education, family size, marital status, two-earner household status, defined benefit pension status, IRA participation, and home ownership. We describe the features of the 401(k) dataset in Table 2.

Given the heavy-tailed distribution of net worth measures, we perform a pre-processing step to remove outliers. Specifically, we eliminate the top and bottom 2.5% of observations, effectively narrowing the range of potential outcomes from  $[-0.5 \times 10^6, 1.5 \times 10^6]$  to  $[-1.4 \times 10^4, 1.34 \times 10^5]$ . This adjustment leaves us with 9,419 observations, which are then evenly distributed between the observational and experimental datasets. We find that this procedure improves the stability of regression and classification algorithms across different random data splits.

This dataset has previously been analyzed using Random Forest algorithms [10]. Consistent with this earlier work, we employ the same models (`RandomForestRegressor` and

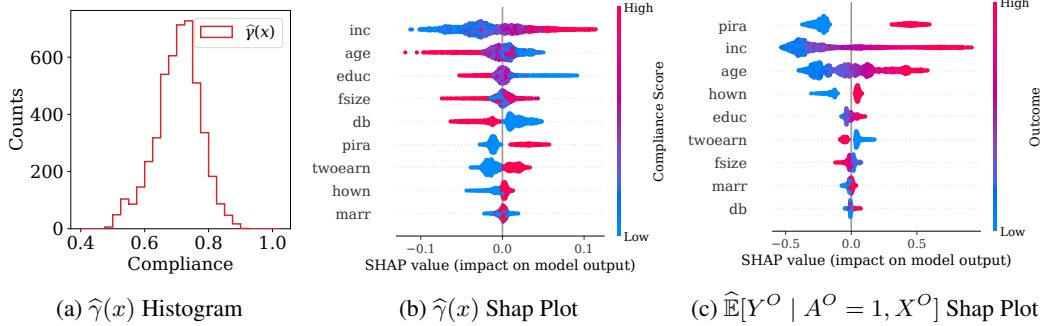


Figure 3: Characteristics of the 401(k) dataset derived from the initial stage of Algorithm 1. (3a): Histogram of compliance scores for  $x \in X^E$ . (3b): Shapley plot [32] for the compliance model in the IV dataset with features arranged in decreasing order by feature importance. (3c): Shapley plot for the estimated outcome model  $\hat{\mathbb{E}}[Y^O | A^O = 1, X^O]$  on the observational dataset with features arranged in decreasing order by feature importance

RandomForestClassifier from scikit-learn) and use identical hyperparameters (`n_estimators = 100`, `max_depth = 6`, `max_features = 3`, `min_samples_leaf = 10`) for various regression and classification tasks outlined in Algorithm 1. For the second stage of Algorithm 1, we use a Lasso regressor from scikit-learn with a penalty of  $\alpha = 0.07$  selected via 5-fold cross-validation.

In Figure 3, we display several characteristics of the 401(k) dataset derived from the first stages of Algorithm 1. In particular, we illustrate the spread in compliance scores in IV dataset, as well as the impact of important features on the predictions of the compliance and outcome models, respectively. As noted in the main text, the compliance scores are relatively large and range between 0.49 and 0.90 (mean=0.70). Furthermore, the primary features influencing the compliance score model include income, age, and education. In contrast, the features impacting the outcome model  $\hat{\mathbb{E}}[Y^O | A^O = 1, X^O]$  are IRA participation, income, and age, with education having a significantly lesser effect. This motivated us to investigate how education influences the variability of derived CATEs.

## D Limitations and Societal Impacts of Our Work

Our methodology hinges on several key assumptions, and violations can significantly affect the accuracy and reliability of our estimates. First, the standard IV assumptions (Assumption 1) must hold. If the instrument directly affects the outcome, is correlated with unobserved confounders, or is weak, our estimates may be biased and unreliable. Some of these issues can be mitigated in experimental settings where the instrument is fully randomized. Additionally, the unconfounded compliance assumption requires that compliance is independent of potential outcomes given the covariates. Violations here can also lead to biased estimates if unrecorded explanatory variables affect both outcomes and compliance. Lastly, our method relies on realizability assumptions regarding the bias function. If these assumptions do not hold, our estimates might be biased.

The societal impacts of our method stem from potential inaccuracies in treatment effect estimates and their subsequent use. Inaccurate treatment effect estimates could lead to a range of adverse outcomes, from a diminished user experience on online platforms to less effective healthcare recommendations, economic and public policies. Furthermore, while accurate estimates can provide substantial benefits, they must be used responsibly to avoid unintended consequences such as privacy concerns or potential biases in decision-making. It is thus crucial to apply these methods with careful consideration of ethical implications and societal impacts.